Table S1: Data used in constructing Fig. 1

wt. %	Na	Mg	Al	Si	S	Cr	Fe	
CI	0.496	9.54	0.84	10.7	5.9	0.262	18.66	(1)
CM	0.412	11.66	1.15	13.01	3.3	0.311	20.57	(2)
CO	0.415	13.77	1.37	15.41	2.0	0.338	23.98	(2)
CV	0.326	14.72	1.62	15.8	2.2	0.347	23.23	(2)
R	0.648	12.81	1.08	16.97	4.07	0.357	24.2	(4)
H	0.64	14.0	1.13	16.9	2.0	0.366	27.5	(3)
L	0.70	14.9	1.22	18.5	2.2	0.388	21.5	(3)
LL	0.70	15.3	1.19	18.9	2.3	0.374	18.5	(3)
EH	0.68	10.6	0.81	16.7	5.8	0.315	29.0	(3)
EL	0.58	14.1	1.05	18.6	3.3	0.305	22.0	(3)
Bulk Earth no Si in core	0.18	15.08	1.62	14.43	0.56	0.41	31.48	(1)
7%Si in core	0.18	15.08	1.62	16.67	0.56	0.41	31.48	(1)

(1) Palme and O'Neill (2014), assumed core fraction 32% with 85% Fe; (2) Wolf and Palme (2001), Na from Kallemeyn and Wasson (1981); (3) Wasson and Kallemeyn (1988) ; (4) Bischoff et al. 2011). All S data (except R-chondrites) are from Wasson and Kallemeyn (1981). Cr is calculated from a CI-bulk Earth Mg/Cr ratio.

Additional literature:

Bischoff, A., Vogel, N., Roszjar J. 2011. The Rumuruti chondrite group. Chemie der Erde 71 (2011) 101–133.

Kallemeyn, G.W., Wasson, J.T. 1981. The compositional classification of chondrites-I. The carbonaceous chondrite groups. Geochimica et Cosmochimica Acta 45, 1217.

Wasson, J.T., Kallemeyn, G.W. 1988. Compositions of Chondrites. Philosophical Transactions of the Royal Society of London Series A 325, 535.

Wolf, D., Palme, H. 2001. The solar system abundances of phosphorus and titanium and the nebular volatility of phosphorus. Meteoritics and Planetary Science 36, 559.

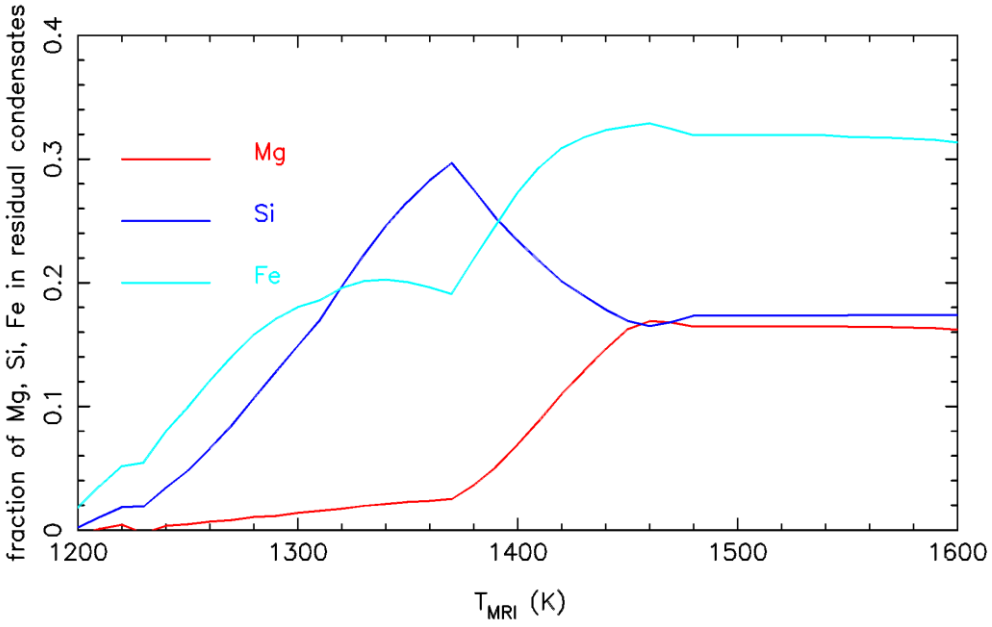

Fig. S1. The mass fractions f^{res}_{Mg}, f^{res}_{Si} and f^{res}_{Fe} of Mg, Si and Fe in residual condensates as a function of temperature of formation of the first planetesimals T_{MRI}. The fraction f^{res}_{Al} is virtually 0 in the showed temperature range, so it is not plotted. These fractions are used in eq. (1) of the main paper.

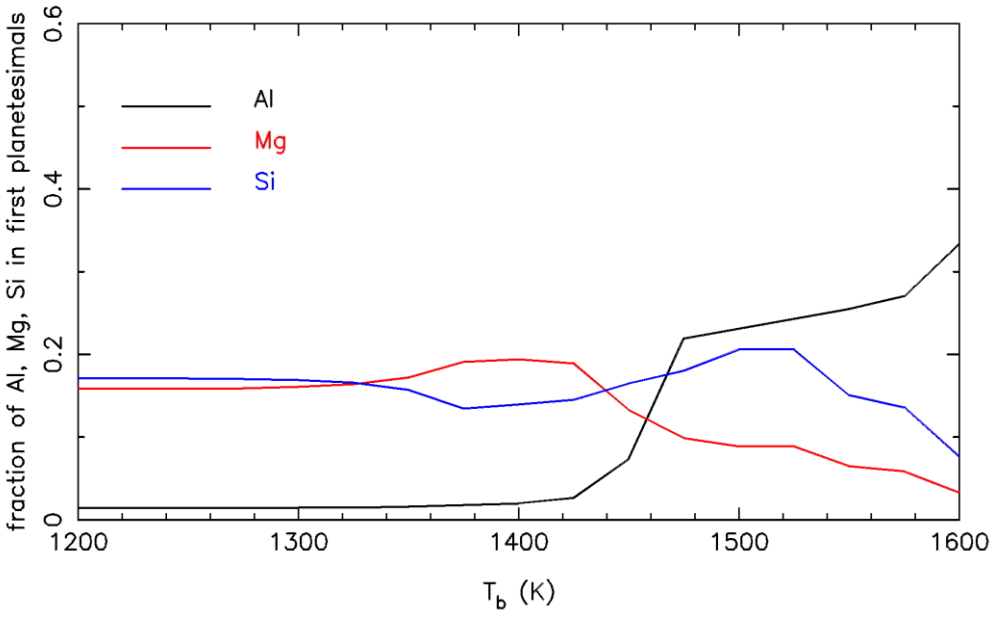

Fig. S2. The mass fractions f^{first}_{Al}, f^{first}_{Mg} *and* f^{first}_{Si} of Al, Mg and Si in first planetesimals as a function of the temperature of formation T_b. The quantities f^{first}_{Al}, f^{first}_{Mg} *and* f^{first}_{Si} are used in the modified eq. (1) in section 4.2 of the main paper.

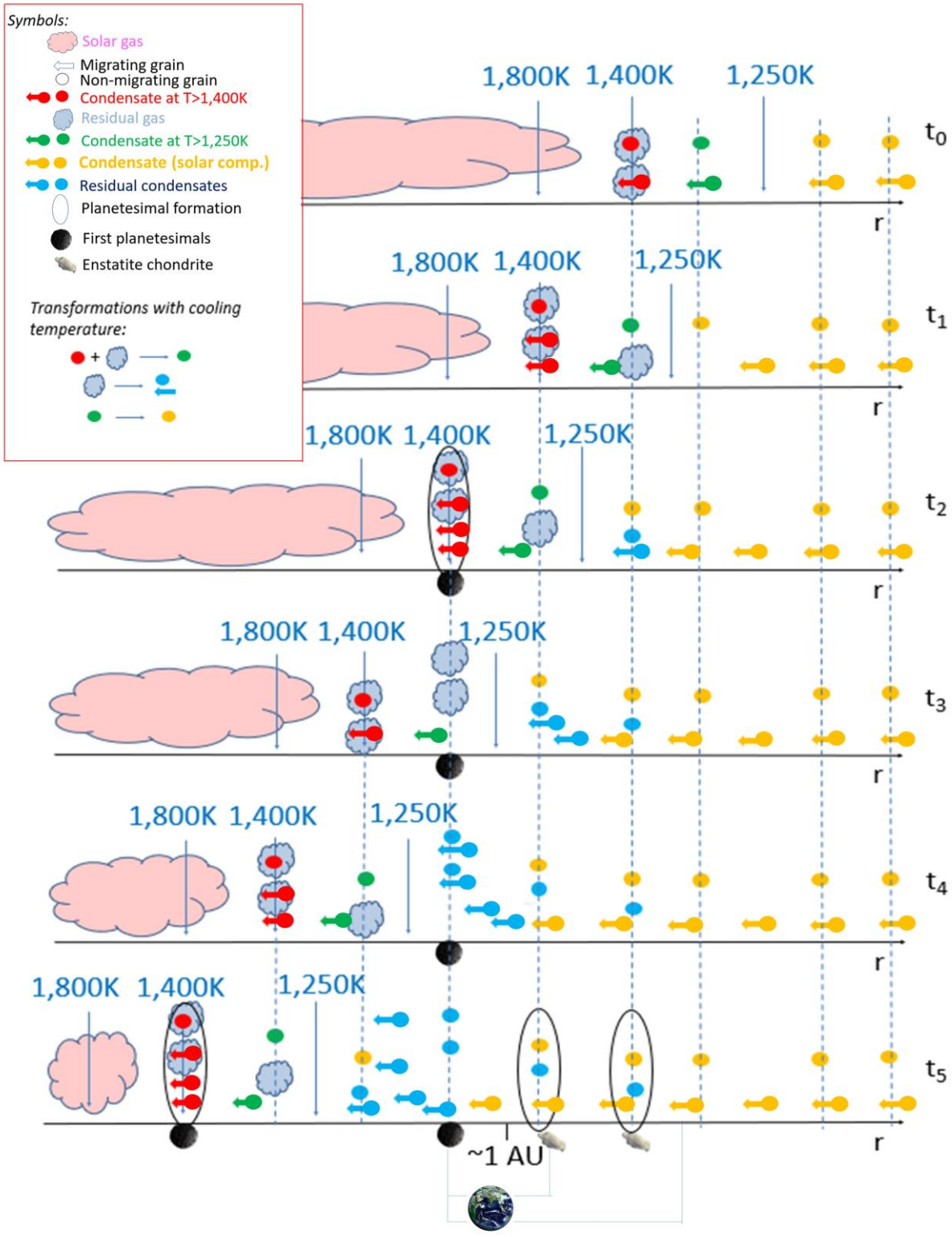

Fig. S3: Sketch of the global evolution of the disk envisioned in this work. The figure shows six time snapshots, from early (t_0) to late (t_5) going from top to bottom. The horizontal axis denotes distance from the star. The three vertical arrows labelled 1,800K, 1,400K, and 1,250K show the locations where the disk temperature has these values. As time progresses from one snapshot to the subsequent one, the disk cools, so the locations of these temperatures shift towards the sun (to the left).

At a temperature greater than 1,800K all material is in a gaseous form and the gas has a solar composition. At lower temperatures some materials have condensed to solids. We indicate in red the grains which followed the equilibrium condensation sequence down to a temperature T=1,400K, in green those which reached temperature T between 1,250K and 1,400K and in orange those which reached temperature T<1,250K. Orange grains have Al/Si and Mg/Si ratios as in CI-chondrites (solar values), although they may miss the volatile component (e.g. water) of CI meteorites if their condensation temperature is higher than a few hundred degrees.
Because we assume to be in a condensation sequence regime, the gas has to drift towards the star more slowly than the temperature lines, so that the parcels of gas cool over time. Thus, for simplification, we assume that the gas is at rest.
Grains drift towards the sun (leftwards) at different speeds, depending on their size[1]. For every condensation event we introduce two pairs of grains. One grain is assumed not to migrate and is represented by a filled dot. The other one instead migrates at the same speed as the temperature lines (filled dot with a left-pointing arrow). This is a simplification, of course, but it captures the real difference existing between grains that migrate faster than (or as fast as) the temperature lines and those migrating less fast.
A guideline for reading the figure could be as follows. Consider first the red dot in the first snapshot (t_0). It has condensed at 1,400K. But because it does not move, it remains in equilibrium with the residual gas. As the temperature decreases (t_1) its composition changes to that of a grain condensed at 1,400K>T>1,250K (green dot on the t_1 panel located vertically below the red dot on the t_0 panel). Then, when the temperature declines further (t_2) it becomes a grain with a solar composition (orange dot). Similarly, the non-migrating green grain in the t_0 panel becomes a solar-composition orange dot in the t_1 panel (placed along the same vertical dashed line), after having been swept by the1,250K line. Now focus on migrating grains, represented by filled dots with arrows. First, consider the red one on the t_0 panel. It migrates with the 1,400K line, leaving behind the residual gas (represented by the gray cloud in the t_1 panel on the vertical dashed line passing through the 1,400K location on the t_0 panel). When the residual gas is swept by the 1,250K line (t_2 panel) it will condense into residual grains (pair of blue dots, one with an arrow, placed vertically along the dashed line). Similarly, the production of residual grains proceeds as more parcels of residual gas cool over time. Finally, look at what happens on the 1,400K line as time progresses. The migrating grain condensed at t_0 (red dot with arrow) remains on the temperature line (remember that this is not due to the specific assumption that the grain migrates at the same speed of the temperature line. Any grain migrating *faster* would remain trapped at the 1,400K line because it corresponds to the transition from a MRI disk to a quiescent disk, hence to a dust trap). So, at time t_1, on the 1,400K line there will be three grains: the migrating one from time t_0, and two new ones, formed at time t_1 because new solar gas is swept by the condensation line. Assuming again that half of the newly condensed grains migrate with the line, at time t_2 there will be 4 grains. This illustrates the pile-up process that eventually can lead to a solid/gas ratio large enough to trigger the streaming instability. Refractory-rich planetesimals can form this way. The figure shows two such events: one at t_2, the other at t_5 in order to illustrate that this process is cyclic and continues as long as the condition holds that the temperature lines migrate faster than the gas.
Late planetesimal formation can also occur when gas is depleted (possibly by photo-evaporation) so that the solid/gas ratio increases due to whatever grains remain in the disk. This is illustrated at time t_5, with the formation of enstatite chondrites from residual (blue) and solar-composition (orange) grains.

In this scenario, as explained in Sect. 4 of the main paper, the Earth builds from a combination of first, refractory-rich planetesimals, solar-composition grains and/or enstatite chondrites, with an excess of refractory material over solar-composition material.

[1]For a description of the drift speed as a function of grain size in different parts of the disk, see for instance Lambrechts and Johansen, 2012, A&A, 544, 32L.

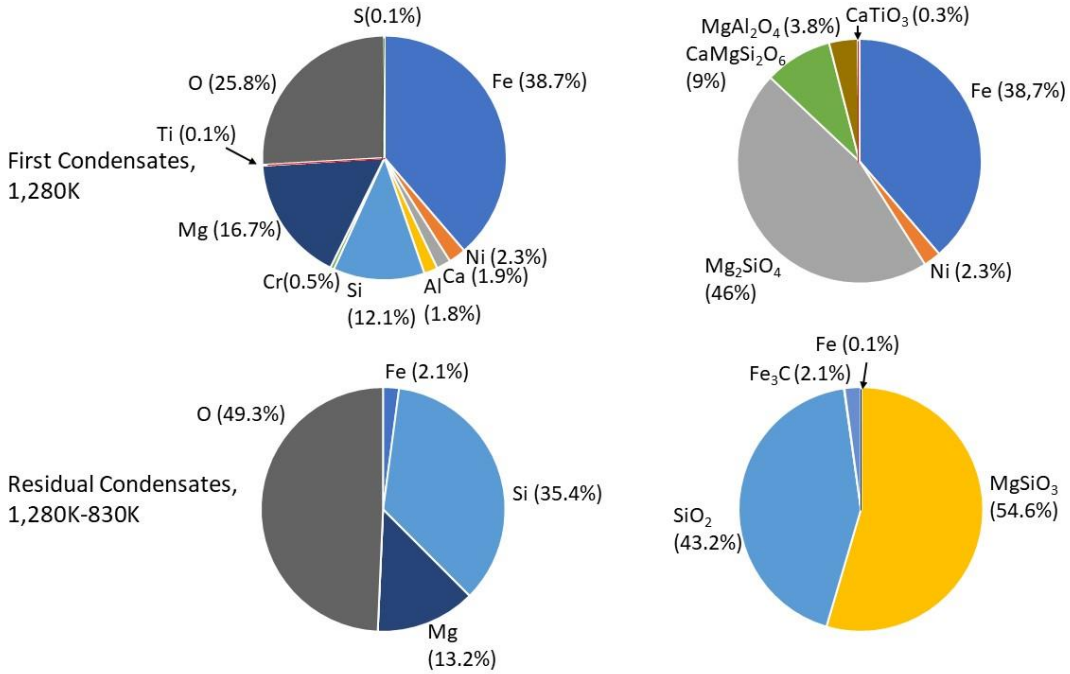

Fig. S4. The same as Fig. 6 of the main text, but computed for C/O=0.9 and T_{MRI}=1,280K

Table S2. Gas species included in the equilibrium condensation calculation from the factsage data base. http://www.crct.polymtl.ca/fact/documentation/

H(g)
H2(g)
C(g)
C2(g)
C3(g)
C4(g)
C5(g)
CH(g)
CH2(g)
CH3(g)
CH4(g)
C2H(g)
C2H2(g)
C2H3(g)
C2H4(g)
C2H5(g)
C2H6(g)
O(g)
O2(g)
O3(g)
OH(g)
H2O(g)
HOO(g)
HOOH(g)
CO(g)
C2O(g)
CO2(g)
C3O2(g)
HCO(g)
H2CO(g)
CH3O(g)
CH3O(g2)
CH3OH(g)
CH2CO(g)
C2H4O(g)
C2H4O(g2)
CH3CH2OH(g)
CH3CH2OH(g2)
COOH(g)
HCOOH(g)
CH3COOH(g)
Na(g)
Na2(g)
NaH(g)
NaO(g)
NaOH(g)
(NaOH)2(g)
Mg(g)
Mg2(g)
MgH(g)
MgO(g)
MgOH(g)
Mg(OH)2(g)
Al(g)
Al2(g)
AlH(g)
AlC(g)
AlC2(g)
Al2C2(g)
AlO(g)
AlO2(g)
Al2O(g)
Al2O2(g)
Al2O3(g)
AlOH(g)
AlOH(g2)
OAlOH(g)
Si(g)
Si2(g)
Si3(g)
SiH(g)
SiH4(g)
Si2H6(g)
SiC(g)
SiC2(g)
Si2C(g)
SiO(g)
SiO2(g)
S(g)
S2(g)
S3(g)
S4(g)
S5(g)
S6(g)
S7(g)
S8(g)
HS(g)
H2S(g)
H2S2(g)
CS(g)
CS2(g)
CH3SH(g)
C2H4S(g)
(CH3)2S(g)
(CH3)2S(g2)
CH3SSCH3(g)
SO(g)
SO2(g)
SO3(g)
SSO(g)
H2SO4(g)
COS(g)
C2H4OS(g)
(CH3)2SO(g)
(CH3)2SO2(g)
Na2SO4(g)
MgS(g)
AlS(g)
Al2S(g)
Al2S2(g)
SiS(g)
SiS2(g)
Ca(g)
Ca2(g)
CaH(g)
CaO(g)
CaOH(g)
Ca(OH)2(g)
CaS(g)
Ti(g)
TiO(g)
TiO2(g)
TiS(g)
Cr(g)
CrO(g)
CrO2(g)
CrO3(g)
CrOH(g)
CrOOH(g)
Cr(OH)2(g)
CrO2OH(g)
CrO(OH)2(g)
Cr(OH)3(g)
CrO2(OH)2(g)
CrO(OH)3(g)
Cr(OH)4(g)
CrO(OH)4(g)
Cr(OH)5(g)
Cr(OH)6(g)
CrS(g)
Fe(g)
FeO(g)
Fe(OH)2(g)
Fe(CO)5(g)
FeS(g)
Ni(g)
NiH(g)
NiO(g)
Ni(OH)2(g)
Ni(CO)4(g)
NiS(g)

Table S3. Pure solid phases included in the equilibrium condensation calculation from the factsage data base. http://www.crct.polymtl.ca/fact/documentation/

C(s)
C(s2)
H2O(s)
Na(s)
NaH(s)
C2Na2(s)
NaO2(s)
Na2O2(s)
Na2O2(s2)
NaOH(s)
NaOH(s2)
Na2CO3(s)
Na2CO3(s2)
Na2CO3(s3)
NaHCO3(s)
Na2CO3(H2O)10(s)
Mg(s)
MgH2(s)
MgC2(s)
Mg2C3(s)
Mg(OH)2(s)
MgCO3(s)
Al(s)
AlH3(s)
Al4C3(s)
Al(OH)3(s)
Al2O3(H2O)(s)
Al2O3(H2O)(s2)
Al2O3(H2O)3(s)
AlCH2NaO5(s)
Si(s)
SiC(s)
SiC(s2)
H2SiO3(s)
H4SiO4(s)
H2Si2O5(s)
H6Si2O7(s)
Mg2Si(s)
Mg3Si2O5(OH)4(s)
Mg3Si4O10(OH)2(s)
Mg7Si8O22(OH)2(s)
Al2SiO5(s)
Al2SiO5(s2)
Al2SiO5(s3)
(Al2O3)(SiO2)2(H2O)2(s)
(Al2O3)(SiO2)2(H2O)2(s2)
Al2Si4O10(OH)2(s)
NaAlSi2O6H2O(s)
NaAl3Si3O12H2(s)
Mg5Al2Si3O10(OH)8(s)
Mg2Al4Si5O18(H2O)(s)
Na2Mg3Al2Si8O22(OH)2(s)
SO3(s)
Na2S(s)
NaS2(s)
Na2S2(s)
Na2S3(s)
Na2SO3(s)
Na2SO4(s)
Na2SO4(s2)
Na2SO4(s3)
Na2SO4(H2O)10(s)
Na3(OH)(SO4)(s)
MgS(s)
MgSO4(s)
MgSO4(H2O)(s)
MgSO4(H2O)6(s)
MgSO4(H2O)7(s)
Al2S3(s)
Al2(SO4)3(s)
Al2(SO4)3(H2O)6(s)
SiS(s)
SiS2(s)
Ca(s)
Ca(s2)
CaH2(s)
CaH2(s2)
CaC2(s)
CaC2(s2)
CaO2(s)
Ca(OH)2(s)
CaCO3(s)
CaCO3(s2)
CaC2O4(H2O)(s)
Mg2Ca(s)
CaMg(CO3)2(s)
Al2Ca(s)
Al4Ca(s)
(CaO)3(Al2O3)(H2O)6(s)
(CaO)4(Al2O3)(H2O)13(s)
CaSi(s)
CaSi2(s)
Ca2Si(s)
(CaO)(SiO2)2(H2O)2(s)
(CaO)3(SiO2)2(H2O)3(s)
(CaO)4(SiO2)6(H2O)5(s)
(CaO)5(SiO2)6(H2O)3(s)
(CaO)6(SiO2)6(H2O)(s)
(CaO)8(SiO2)6(H2O)3(s)
(CaO)10(SiO2)12(H2O)11(s)
(CaO)10(SiO2)12(H2O)21(s)
(CaO)12(SiO2)6(H2O)7(s)
Ca2Mg5Si8O22(OH)2(s)
CaAl2Si2O7(OH)2(H2O)(s)
CaAl4Si2O10(OH)2(s)
CaAl14Si22O60(OH)12(s)
Ca2Al3Si3O12(OH)(s)
Ca2Al3Si3O12(OH)(s2)
(CaO)2(Al2O3)2(SiO2)8(H2O)7(s)
CaS(s)
CaSO3(s)
CaSO4(s)
CaSO4(s2)
CaSO3(H2O)2(s)
CaSO4(H2O)2(s)
(CaSO3)2(H2O)(s)
(CaSO4)2(H2O)(s)
Ti(s)
Ti(s2)
TiH2(s)
CTi(s)
TiO(s)
TiO(s2)
TiAl(s)
TiAl3(s)
SiTi(s)
Si2Ti(s)
TiS(s)
TiS2(s)
TiS3(s)
Ti2S(s)
Ti2S3(s)
Cr(s)
Cr3C2(s)
Cr4C(s)
Cr7C3(s)
Cr23C6(s)
CrO2(s)
CrO3(s)
Cr5O12(s)
Cr8O21(s)
Cr(CO)6(s)
CrSi2(s)
Cr3Si(s)
Cr5Si3(s)
Cr2(SO4)3(s)
Fe(s)
Fe(s2)
Fe3C(s)
Fe3C(s2)
Fe(OH)2(s)
Fe(OH)3(s)
Fe2O3(H2O)(s)
FeCO3(s)
FeAl3(s)
FeSi(s)
FeSi2(s)
Fe3Si(s)
Fe3Si7(s)
Fe7Si8O22(OH)2(s)
FeSO4(s)
Fe2(SO4)3(s)
FeSO4(H2O)7(s)
FeTi(s)
Fe2Ti(s)
Ni(s)
Ni2H(s)
Ni3C(s)
NiOOH(s)
Ni(OH)2(s)
NiO2(H2O)(s)
NiCO3(s)
MgNi2(s)
NiAl(s)
Al3Ni(s)
Ni2Al3(s)
Ni3Al(s)
NiSi(s)
Ni2Si(s)
Ni7Si13(s)
NiSO4(s)
NiSO4(H2O)(s)
NiSO4(H2O)6(s)
NiSO4(H2O)7(s)
Ni4SO4(OH)6(s)
NiTi(s)
NiTi2(s)
Ni3Ti(s)
(NiO)(TiO2)(s)
NiTi2O5(s)
Ni2TiO4(s)
S(s)
S(s2)
Cr2S3(s)
FeS(s)
FeS2(s)
Fe7S8(s)
Fe9S10(s)
Fe10S11(s)
Fe11S12(s)
FeCr2S4(s)
NiS(s)
NiS2(s)
Ni3S2(s)
Ni3S4(s)

Ni7S6(s)
Ni9S8(s)
MgO(s)
Al2O3(s)
Al2O3(s2)
Al2O3(s3)
Al2O3(s4)
SiO2(s)
SiO2(s2)
SiO2(s3)
SiO2(s4)
SiO2(s5)
SiO2(s6)
SiO2(s7)
SiO2(s8)
MgSiO3(s)
MgSiO3(s2)
MgSiO3(s3)
MgSiO3(s4)
MgSiO3(s5)
MgSiO3(s6)
MgSiO3(s7)
Mg2SiO4(s)
Mg2SiO4(s2)
Mg2SiO4(s3)
Al2Si2O7(s)
NaAlSiO4(s)
NaAlSiO4(s2)
NaAlSi2O6(s)
NaAlSi3O8(s)
NaAlSi3O8(s2)
Mg4Al10Si2O23(s)
Mg3Al2Si3O12(s)
Mg2Al4Si5O18(s)
CaO(s)
CaAl2O4(s)
CaAl4O7(s)
CaAl12O19(s)
Ca3Al2O6(s)
CaMg2Al16O27(s)
Ca2Mg2Al28O46(s)
Ca3MgAl4O10(s)
CaSiO3(s)
CaSiO3(s2)
Ca2SiO4(s)
Ca2SiO4(s2)
Ca2SiO4(s3)
Ca3SiO5(s)
Ca3Si2O7(s)
CaMgSi2O6(s)
Ca2MgSi2O7(s)
Ca3MgSi2O8(s)
CaAl2SiO6(s)
CaAl2Si2O8(s)
CaAl2Si2O8(s2)
Ca2Al2SiO7(s)
Ca3Al2Si3O12(s)
TiO2(s)
TiO2(s2)
Ti2O3(s)
Ti2O3(s2)
Ti3O5(s)
Ti3O5(s2)
Ti4O7(s)
Ti5O9(s)
Ti6O11(s)
Ti7O13(s)
Ti8O15(s)
Ti9O17(s)
Ti10O19(s)
Ti20O39(s)
MgTiO3(s)
Mg2TiO4(s)
Mg2TiO4(s2)
MgTi2O5(s)
Al2TiO5(s)
Al4TiO8(s)
CaTiO3(s)
CaTiO3(s2)
Ca2Ti2O5(s)
Ca2Ti2O5(s2)
Ca3Ti2O6(s)
Ca3Ti2O7(s)
Ca5Ti4O13(s)
CaSiTiO5(s)
Cr2O3(s)
CaCr2O4(s)
CaCr2O4(s2)
(Ca2Cr3)Cr10O20(s)
(CaCr)Si4O10(s)
Ca3Cr2Si3O12(s)
Fe2O3(s)
Fe2O3(s2)
Fe2O3(s3)
Al2Fe2O6(s)
FeSiO3(s)
FeSiO3(s2)
FeSiO3(s3)
Fe2SiO4(s)
Fe2SiO4(s2)
Fe2SiO4(s3)
Fe2Al4Si5O18(s)
Fe3Al2Si3O12(s)
CaFe2O4(s)
Ca2Fe2O5(s)
CaFe4O7(s)
CaFeSi2O6(s)
Ca2FeSi2O7(s)
Ca3Fe2Si3O12(s)
(FeO)(TiO2)(s)
FeTi2O4(s)
FeTi2O5(s)
(FeO)2(TiO2)(s)
NiO(s)
Ni2SiO4(s)
NiCaSi2O6(s)

Note: (s2, s3, …) standing for different polymorphs of the (s) phase